Electronic Supporting Information for

"Toward Steric Control of Guest Binding Modality: a Tripodal Co(II) Complex Exhibiting Cation Binding and Zero-Field Relaxation"

Tarik J. Ozumerzifon, Indrani Bhowmick, William C. Spaller, Anthony K. Rappé, and Matthew P. Shores

Contents

Experimental Details

2-formyl-5-(N-*tert*-butyl)-nicotinamide[1] and *cis*,*cis*-1,3,5-triaminocyclohexane (tach)[2] were prepared according to literature. All reactions were performed under ambient conditions (room temperature, normal benchtop atmosphere) unless otherwise stated. Syringe filters were purchased from VWR International and were fitted with 0.2 μm PTFE membranes. Absorption

spectra were obtained with a Hewlett-Packard 8453 spectrometer in quartz cuvettes with a 1 cm path length. Infrared spectra were measured with a Nicolet 380 FT-IR spectrometer. Mass spectrometry measurements were performed in the positive ion mode on a Thermo LTQ mass spectrometer equipped with an analytical electrospray ion source and a quadrupole ion trap mass analyzer at 175 °C. Diethyl ether (Et_2O) and acetonitrile (MeCN) were sparged with nitrogen, passed through an alumina column and degassed prior to use. All other chemicals were purchased from commercial vendors and used as received. Elemental analyses were performed by Robertson Microlit Laboratories, Inc. in Madison, NJ.

Magnetic measurements: Direct current (dc) magnetic data were collected for **1** and **2** using a Quantum Design MPMS XL SQUID magnetometer between 1.8 and 300 K and 0 to 5 T. The ac magnetic measurements were performed between 1-1500 Hz using a 4 Oe ac oscillating field. Powdered microcrystalline samples were loaded into polyethylene bags (1 cm × 1.5 cm), sealed, and inserted into drinking straws for measurements. Ferromagnetic impurities were checked through a variable field measurement (0 to 10000 or 20000 Oe) of the magnetization at 100 K; linear fits of the *M* versus *H* data between 0 and 10000 Oe (Figures S4−S5) indicates the absence of ferromagnetic impurities. Magnetization measurements were collected at 2 K at applied fields ranging from 0 to 50 kOe (Figure S6). Data were corrected for the diamagnetic contributions of the sample holder and bag by subtracting empty containers; corrections for the sample were calculated from Pascal's constants.[3] Fits of magnetic susceptibility data were performed using PHI[4] according to the following Hamiltonian:

$$\widehat{H} = \sum D_i\left[S_{z,i}^2 - 1/3S_i(S_i+1) + E_i/D_i\left(S_{x,i}^2 - S_{y,i}^2\right)\right] + \sum g_{xx,i}\beta\check{S}_{x,i}\cdot\widetilde{B_x} + g_{yy,i}\beta\check{S}_{y,i}\cdot\widetilde{B_y} + g_{zz,i}\beta\check{S}_{z,i}\cdot\widetilde{B_z}$$

Single crystal X-ray diffraction: Crystallographic parameters for the compounds are listed in Table S1. All crystals were coated in Paratone oil for data collection. The crystals were supported on Cryoloops, and then mounted on a Bruker Kappa Apex 2 CCD diffractometer under a stream of dinitrogen. Mo Kα radiation and a graphite monochromator were used for data collection. Initial lattice parameters were determined from reflections found in 36 frames. Data sets were collected targeting complete coverage and fourfold redundancy. Data were integrated and corrected for absorption effects with APEX 2 software.[5] Structures were solved and refined with the SHELXTL software package.[6] Unless noted otherwise, thermal parameters for all fully occupied, nonhydrogen atoms were refined anisotropically; hydrogen atoms were added at the ideal positions and were refined using a riding model where the thermal parameters were set at 1.2 times those of the attached carbon or nitrogen atom (1.5 times that for methyl protons).

Compound **2** crystallizes with partial occupancy and disorder of solvate molecules; this disorder was removed using SQUEEZE (model A). This process removed electron density corresponding to 73.81 electrons for a void space of 219.5 $Å^3$ per unit cell. An explicit model (B), where the remaining electron density was modeled as two acetonitrile molecules (one at 0.333 occupancy, one at 0.666 occupancy) and one diethyl ether molecule (at 0.25 occupancy), gave slightly better agreement factors (R_1 = 0.0583), but with a larger number of parameters, such that model B was not a statistical enhancement of model A. In addition, relative to model A, the explicit disorder model (B) gave a disproportionate number of alerts in the checkcif due to overparameterization. Finally, three acetonitrile molecules and 0.75 ether molecules per unit cell correspond roughly to 97.5 electrons (275 $Å^3$, assuming 25 $Å^3$/atom), higher than expected from the SQUEEZE analysis. Attempts to decrease the occupancy of any of the solvent sites significantly deteriorate agreement with the data. Thus, the SQUEEZEd model (A) was used as the final model.

Also in the structure of **2**, the H_2O molecule present on the Na ion lies off of the three-fold rotational axis, so the occupancy of the O atom was set to 0.333. Addition of H atoms causes the anisotropic thermal parameters of the O atom to become non positive definite, so the H atoms were omitted from the final model.

Full information has been deposited with the CCDC under registry numbers 1527921 - 1527923 for **1**, **2** and the bis(triiodido) salt, $[LCo](I_3)_2$.

Syntheses of Cobalt(II) Salts

$[LCo][CoCl_4]$ (1)

To a solution of tach (0.060 g, 0.47 mmol) in MeOH (2 mL) was added a solution of 2-formyl-5-(N-*tert*-butyl)-nicotinamide (0.300 g, 1.44 mmol) in MeOH (2 mL), and the resulting mixture was stirred at 23 °C for 30 minutes in the presence of 3Å molecular sieves. A solution of $CoCl_2$ (0.060 g, 0.47 mmol) in MeOH (5 ml) was then added, and the resulting orange solution was stirred at 23 °C for an additional hour. Then, diethyl ether (10 mL) was added to precipitate the crude product, which was isolated by vacuum filtration. Diffraction quality crystals were obtained from a diethyl ether diffusion into a concentrated solution of the crude product in methanol, giving **1** (0.091 g, 19% yield) as green needle-like crystals. **UV-Vis**, MeOH, λ, nm (ε, $M^{-1}cm^{-1}$): 226 (36200), 274 (21200), 355 (2300), 527 (140). **MS** (ESI^+): *m/z* calc'd for $(M - CoCl_4 + Cl)^+$ $[C_{39}H_{51}N_9O_3ClCo]^+$: 787.31, found 787.42, *m/z* calc'd for $(M - CoCl_4)^{2+}$ $[C_{39}H_{51}N_9O_3Co]^{2+}$: 376.17, found 376.25. **Anal.** calc'd ($C_{39}H_{51}N_9O_3Co_2Cl_4$ + 2(CH_4O): C: 48.39%, H: 5.84%, N: 12.39%, found C: 48.04%, H: 5.58%, N: 12.36%.

{Na[LCo]}$(BPh_4)_3$ (2)

To a solution $NaBPh_4$ (0.220 g, 0.67 mmol) in MeOH (2 mL) was added dropwise a solution of **1** (0.024 g, 0.024 mmol) in MeOH (2 mL), immediately forming a suspension, which was stirred at 23 °C for 12 h. The reaction mixture was then filtered to isolate crude **2**, and diffraction quality crystals were grown by diethyl ether diffusion into a concentrated acetonitrile solution of the crude product, giving yellow block-like crystals of **2** (0.013 g, 30% yield). **UV-Vis**, MeCN, λ, nm (ε, $M^{-1}cm^{-1}$): 244 (92500), 276 (30500), 410 (4500). **MS** (ESI^+): *m/z* calc'd for (M - Na - $2BPh_4)^+$ $[C_{63}H_{71}N_9O_3BCo]^+$: 1071.51, found 1071.25, *m/z* calc'd for (M - Na - $3BPh_4)^{2+}$ $[C_{39}H_{51}N_9O_3Co]^{2+}$: 376.17, found 376.25. **Anal.** calc'd for ($C_{111}H_{111}B_3N_9O_3Co$ + 1(C_2H_3N) + 1($C_4H_{10}O$)+ 2.5(H_2O)): C: 74.21%, H: 6.87%, N: 7.40%, found C: 74.00%, H: 6.56%, N: 7.54%.

Discussion of reaction of L with CoI_2

L was generated *in-situ* in an identical manner as outlined in the syntheses of **1** and **2** except the reaction was performed in a dinitrogen filled glovebox (MBRAUN Labmaster 130): to a solution of tach (0.020 g, 0.15 mmol) in MeOH (3 mL) was added a solution of 2-formyl-5-(N-*tert*-butyl)-nicotinamide (0.090 g, 1.44 mmol) in MeOH (2 mL). The resulting mixture was stirred at 23 °C in the presence of 3Å molecular sieves. After 30 minutes, a solution of CoI_2 (0.049 g, 0.15 mmol) in MeOH (5 ml) was added and the resulting brown mixture was stirred for 12 h at 23 °C. Then, the mixture was passed through a syringe filter and the filtrate concentrated *in vacuo*, and X-ray diffraction quality crystals were obtained from a diethyl ether diffusion into a concentrated solution of the acetonitrile filtrate, giving 0.056 g of brown crystals. Structural analysis shows the formation of the triiodide salt of the tach-derived iminopyridine cobalt complex (see crystallography section, Figure S3). Analysis of the crystalline product *via* mass spectrometry is consistent with the expected formulation: *m/z* calc'd for $(M+I)^+$ $[C_{39}H_{51}N_9O_3Co + I]^+$, 879.25, found 879.08; *m/z* calc'd for (M - $2I_3)^{2+}$, 376.17, found 376.25. Bulk purity combustion analyses, however, fail to confirm absolute purity of this compound and efforts to further purify this species have been unsuccessful. Preliminary magnetic susceptibility studies suggested incomplete conversion of iodide to triiodide. However, efforts to fully convert iodide to triiodide using excess iodine (as has been shown previously for $[Co(12\text{-crown-}4)_2(I_3)_2)$[7] do not afford complete reaction (0.0036 g on a 0.046 mmol scale, 0.070 g theoretical yield) to form the triiodide salt. Therefore, the magnetic properties of this species will not be discussed.

IR Spectroscopy

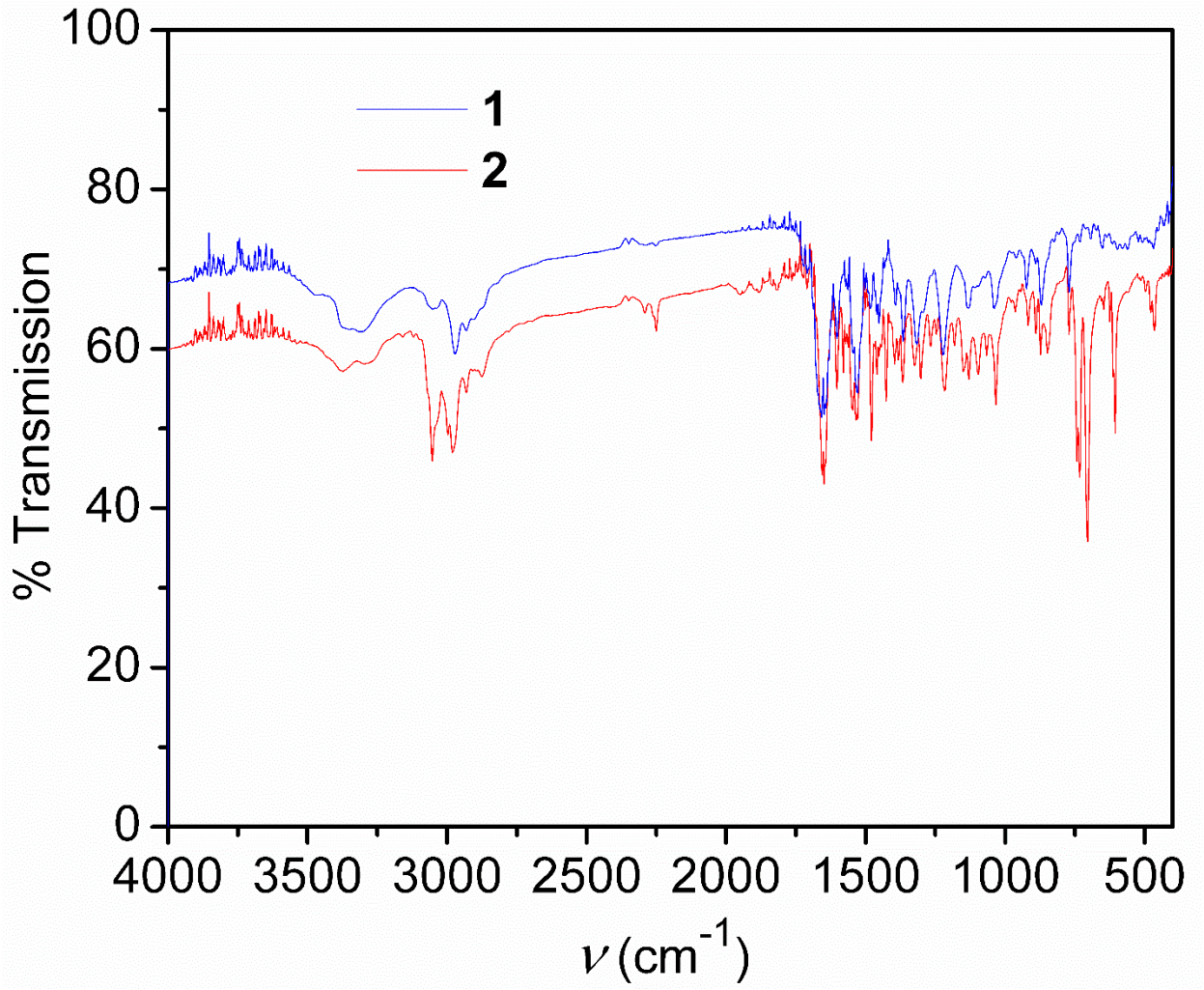

Figure S1. Stacked IR spectra of 1-2. Spectra were obtained using KBr pellets.

UV-Vis Spectroscopy

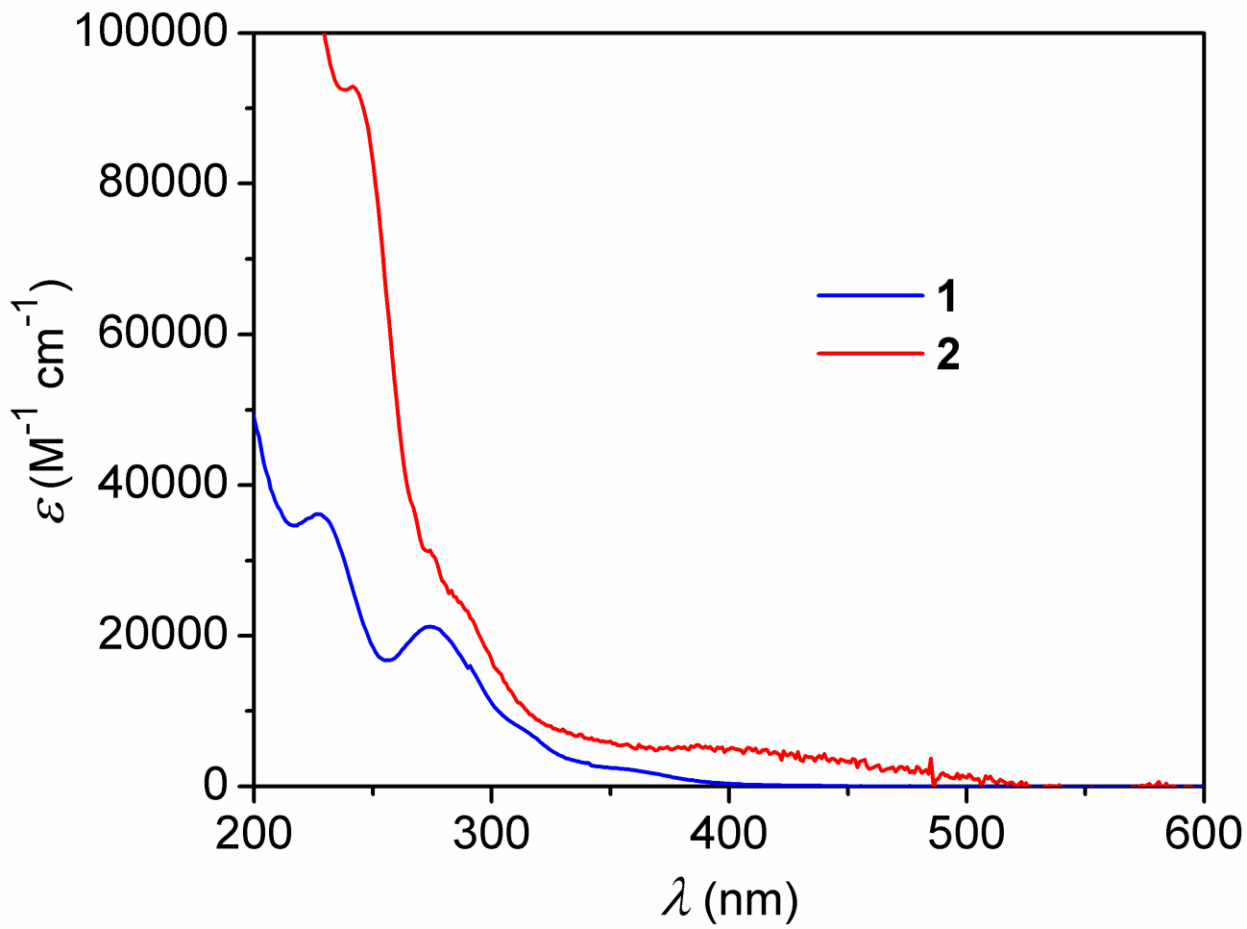

Figure S2. Stacked UV-Vis spectra of 1-2. Spectra were taken in either MeOH (for **1**) or MeCN (for compound **2**).

Crystallography

Table S1. Crystallographic parameters for 1, 2 and $[LCo](I_3)_2$.[a]

	1[b]	**2**	**$[LCo](I_3)_2$**
Formula	$C_{41}H_{58}N_9O_5Co_2Cl_4$	$C_{115}H_{121}B_3N_{10}O_{4.5}CoNa$	$C_{43}H_{61}N_9O_4CoI_6$
Formula weight	1016.62	1749.43	1588.34
Color, habit	green needle	yellow block	brown block
T (K)	120	120	120
Space group	$P\bar{1}$	$R3c$	P $2_1/c$
Z	2	6	4
a (Å)	9.8899(12)	23.7294(15)	23.899(2)
b (Å)	10.4071(13)	23.7294(15)	17.3157(15)
c (Å)	25.652(3)	34.604(3)	13.5491(13)
α (°)	83.322(4)	90	90
β (°)	87.485(5)	90	95.028(3)
γ (°)	65.134(4)	120	90
V (Å^3)	2379.2(5)	16875(3)	5583.0(9)
d_{calc} (g cm^{-3})	1.419	1.033	1.890
GOF	1.042	1.066	1.147
R_1, wR_2[c] (%)	4.67, 13.40	6.04, 15.10	6.11, 13.05

[a] Obtained with graphite-monochromated Mo Kα (λ = 0.71073 Å) radiation.
[b] Unit cell obtained for tetrabromocobaltate salt, $[LCo][CoBr_4]$: a = 9.94 Å, b = 10.47 Å, c = 25.75 Å, α = 92.65°, β = 92.17°, γ = 115.56°, V = 2409 Å^3, based on the collection of 36 frames.
[c] $R_1 = \Sigma\,||F_o| - |F_c||/\Sigma|F_o|$, $wR_2 = \{\Sigma[w(F_o^2 - F_c^2)^2]/\Sigma[w(F_o^2)^2]\}^{1/2}$ for $F_o > 4\sigma(F_o)$.

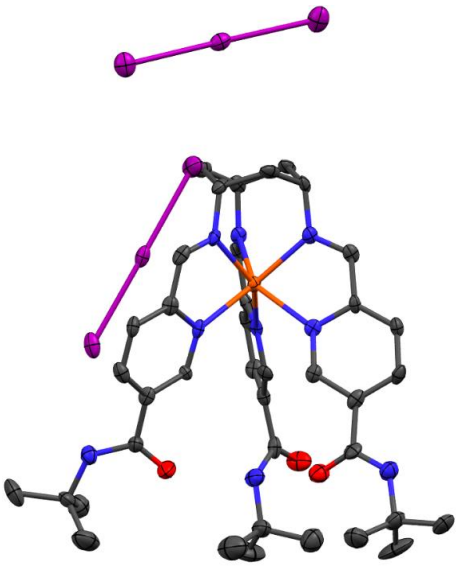

Figure S3. X-ray crystal structure of $[LCo](I_3)_2$. Thermal ellipsoids have been rendered at 40% probability. Orange, red, blue, grey, and purple ellipsoids represent Co, O, N, C and I atoms, respectively. One co-crystallised diethyl ether molecule has been omitted for clarity.

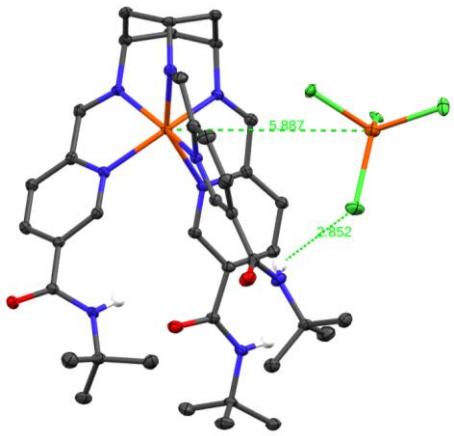

Figure S4. Short contacts in 1. The H-bond between one chlorine in the tetrachlorocobaltate anion and an adjacent amide N-H (distance 2.852(1) Å). The intermolecular Co-Co distance is 5.862(1) Å.

Ferromagnetic Impurity Check

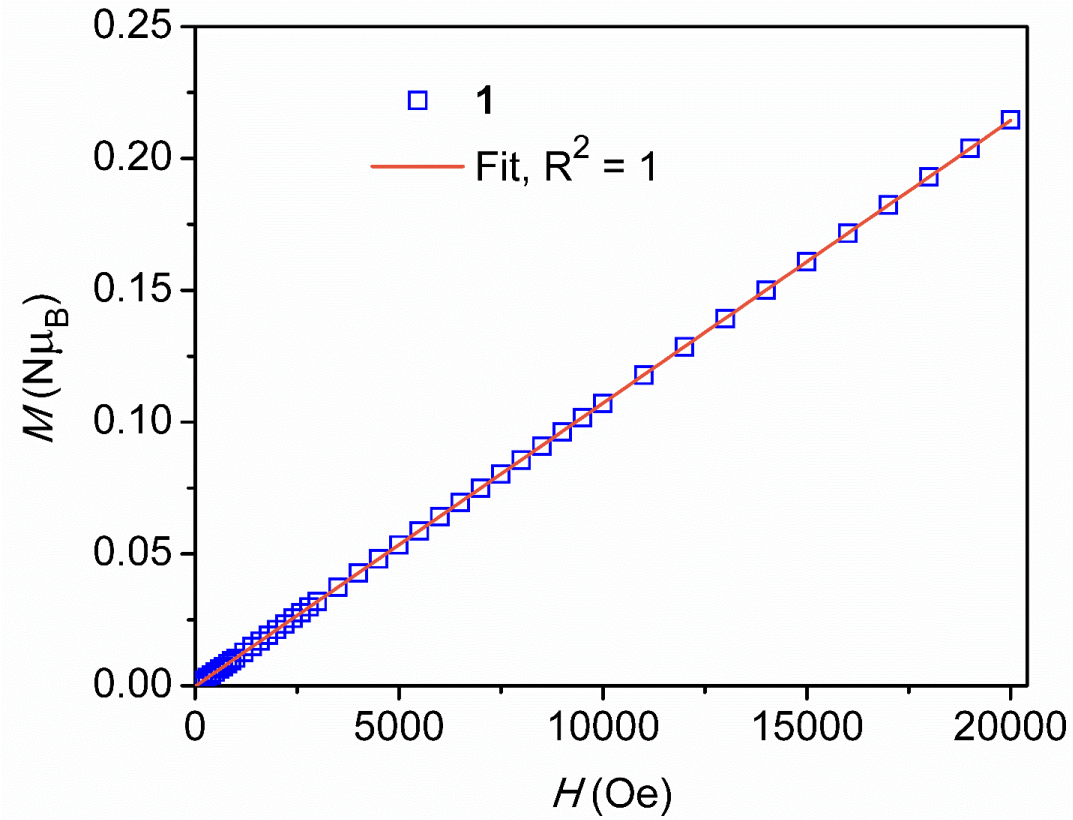

Figure S5. Field dependence of magnetization for 1 collected at 100 K. Fit: $y = 1.07\times10^{-5}(x) - 1.84\times10^{-4}$ ($R^2 = 1$).

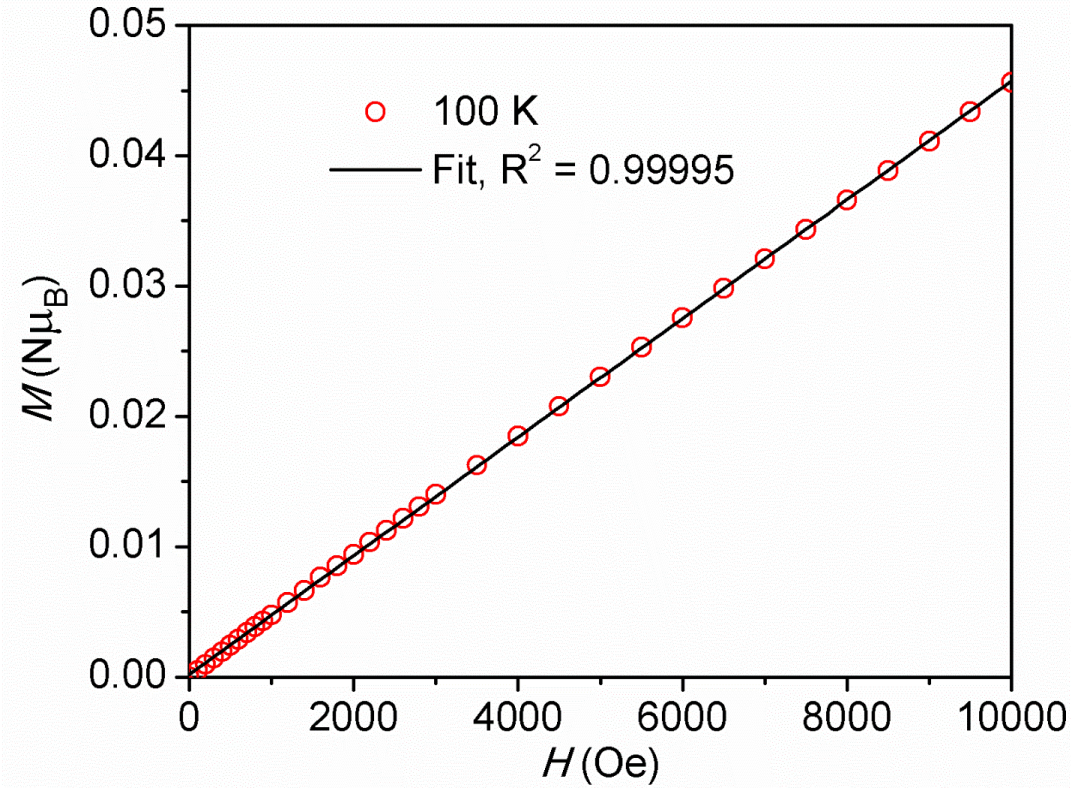

Figure S6. Field dependence of magnetization for 2 collected at 100 K. Fit: $y = 4.55\times10^{-6}(x) - 2.02\times10^{-4}$ ($R^2 = 0.99995$).

Saturation Experiments

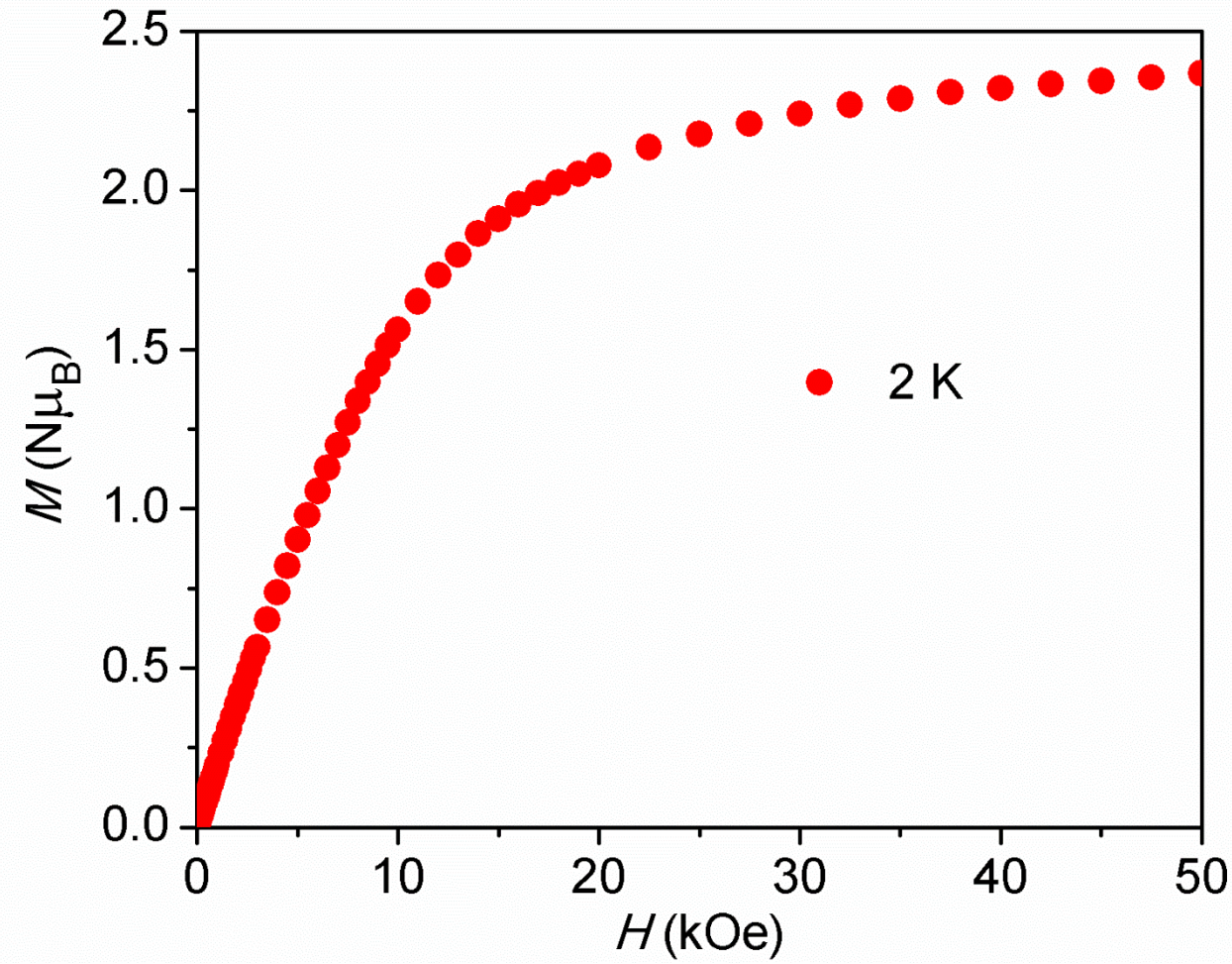

Figure S7. Field dependence of magnetization for 2 collected at 2 K.

1/χ vs. T for 1

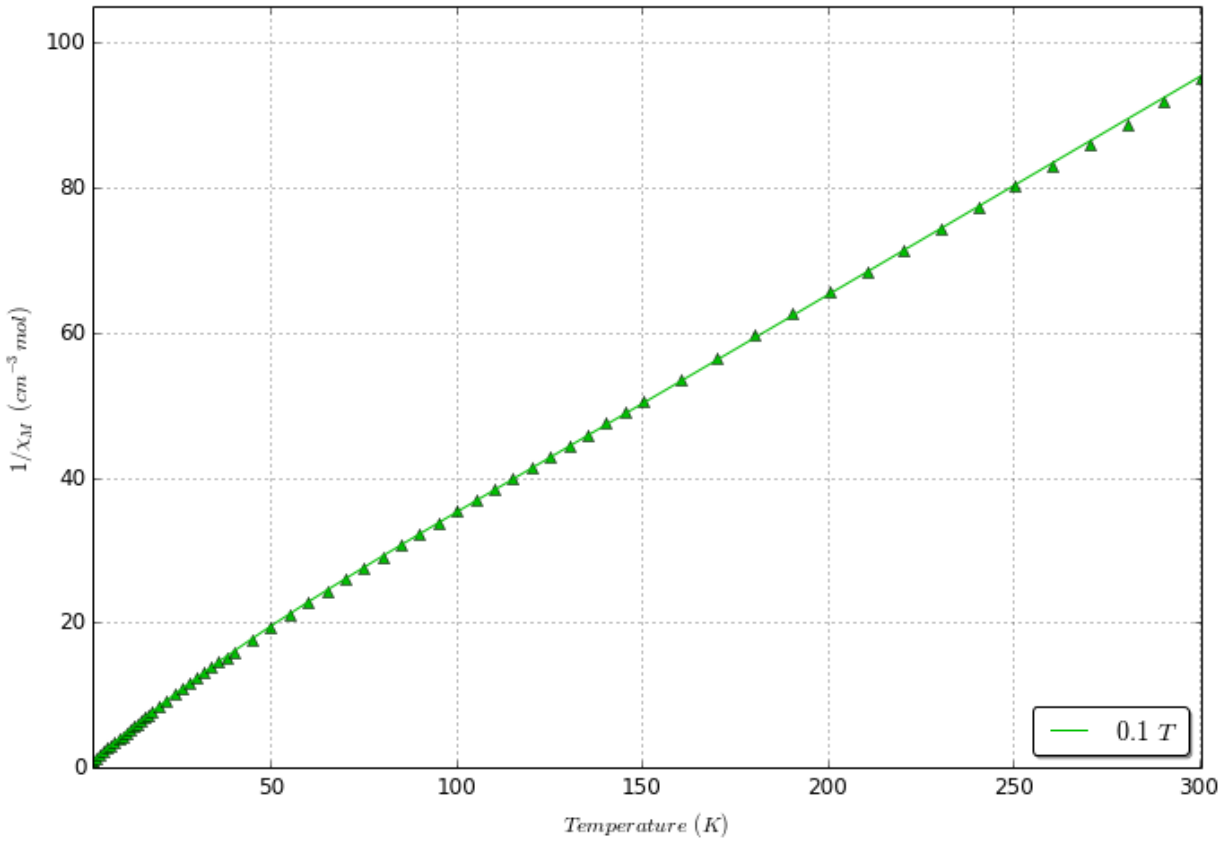

Figure S8. 1/χ vs. T of 1.

Best fit acquired from PHI[4] as described in the manuscript. Θ = 0.49 K (obtained from linear fit to 150-300 K data, not shown here).

Table S2. Magnetic properties acquired by fitting susceptibility data for 1 and 2.

*This fit is included in the manuscript (Table 2)

Compound	*g*	*D* (cm^{-1})	*E* (cm^{-1})	z*J* (cm^{-1})	TIP ($cm^3\ mol^{-1}$)	R^2
1*	2.84	-11.0	0.0084	-	-	0.9933
1	2.84	5.29	5.29	-0.0013	-	0.9999
2*	2.63 (⊥) 2.80 (∥)	-75.8	0.00090	-	0.000500	0.9999
2	2.63 (⊥) 2.80 (∥)	-76.0	0.013	-0.0043	0.000500	0.9999
2	2.84 (iso)	-163	0.011	-	-	0.8931

Reduced Magnetization

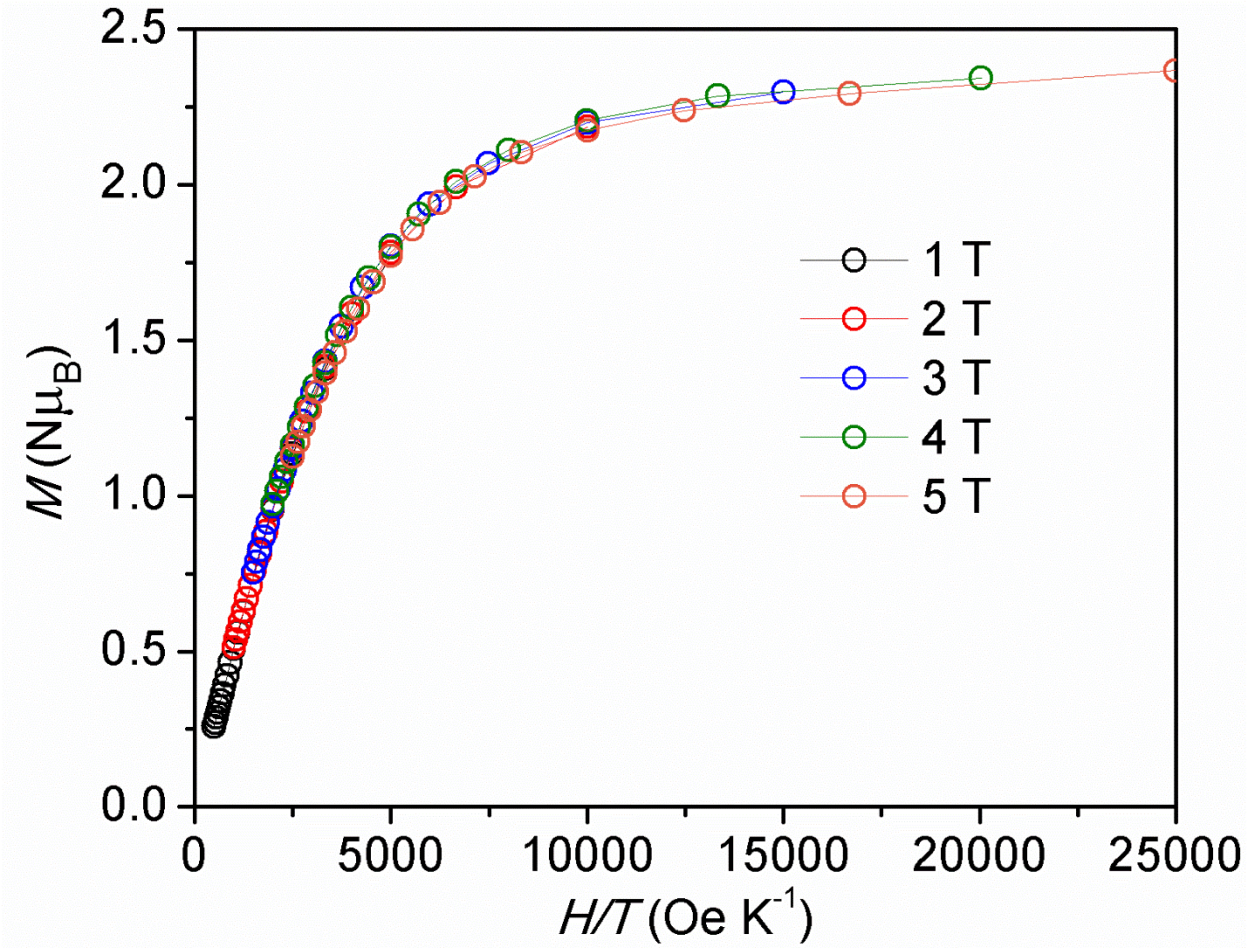

Figure S9. Reduced magnetization of 2. The connecting lines are guides for the eye.

Field Scan

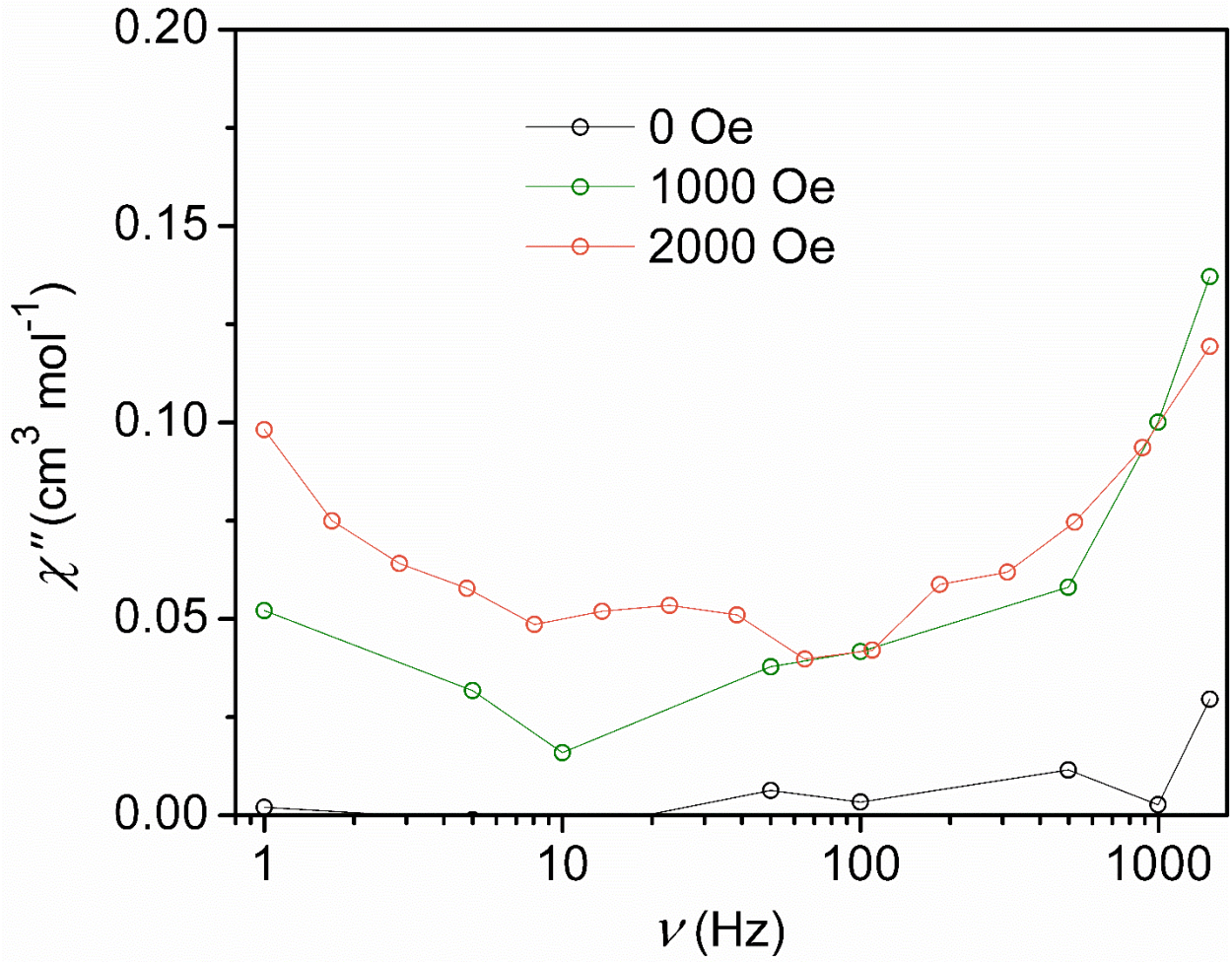

Figure S10. Field scan of 1. Application of 0, 1000 and 2000 Oe dc fields do not result in the detection of an out-of-phase susceptibility (χ'') response (4 Oe oscillating field). Lines are guides for the eye.

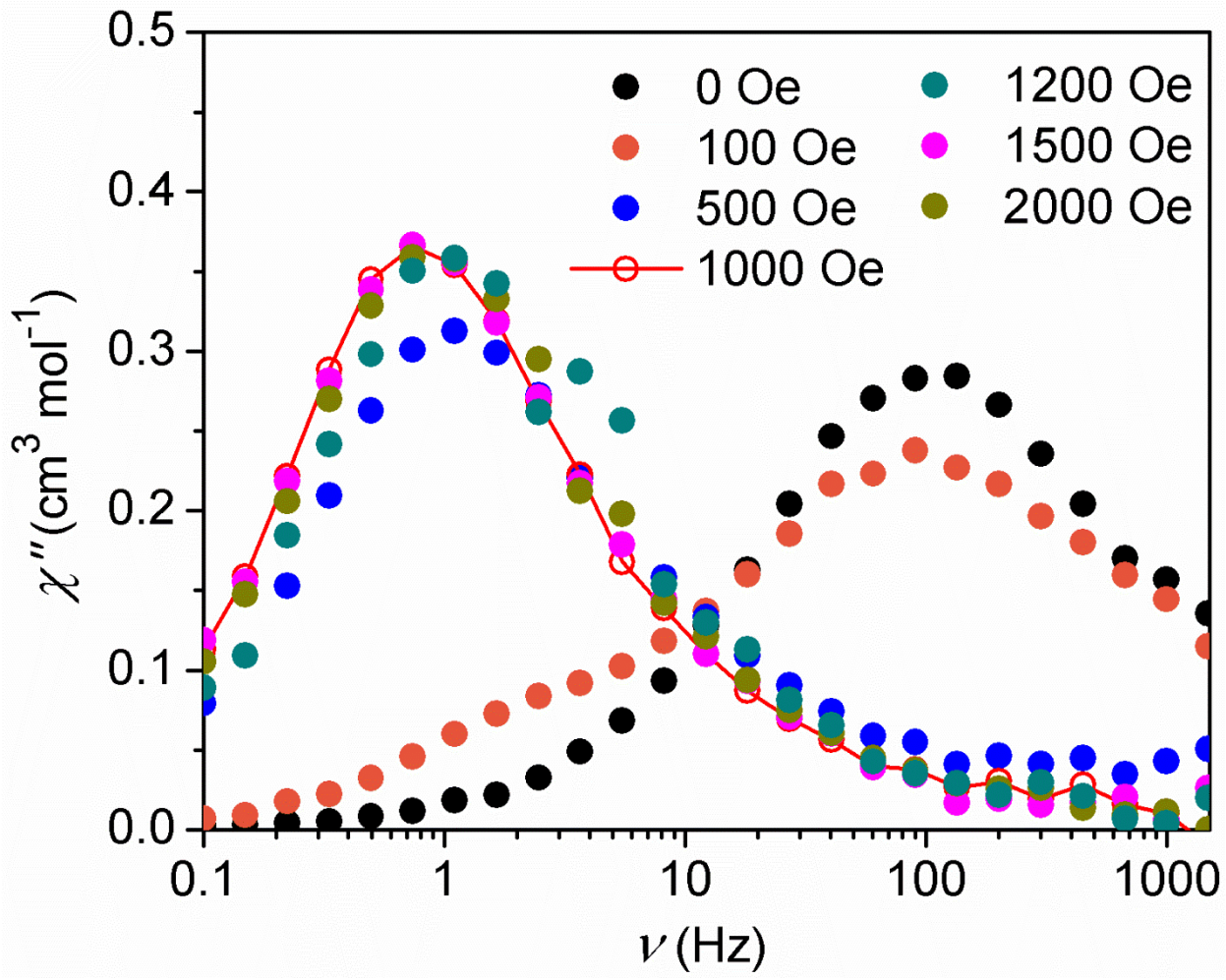

Figure S11. Field scan of 2. Optimal field is shown by solid red line (guide for the eye). Note the complete suppression of the higher frequency relaxation process upon application of sufficiently large dc field.

In-phase susceptibility (χ') vs. frequency for 2

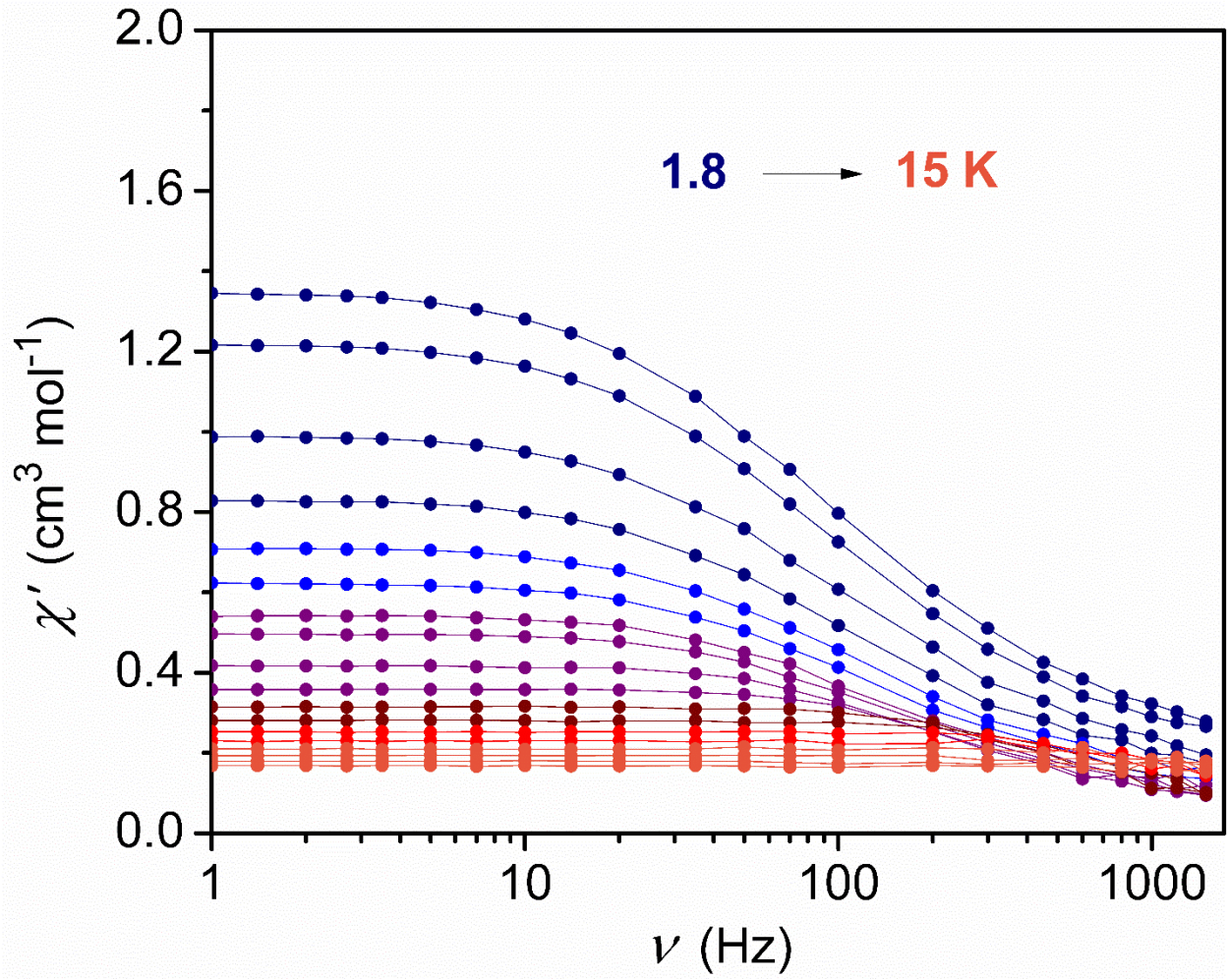

Figure S12. χ' vs. v under no applied DC field for 2.

The temperature was increased in 0.5 K increments from 2 K to 5 K, and 1 K increments from 6 K to 13 K. Data were acquired using an oscillating field of 4 Oe. The lines are guides for the eye.

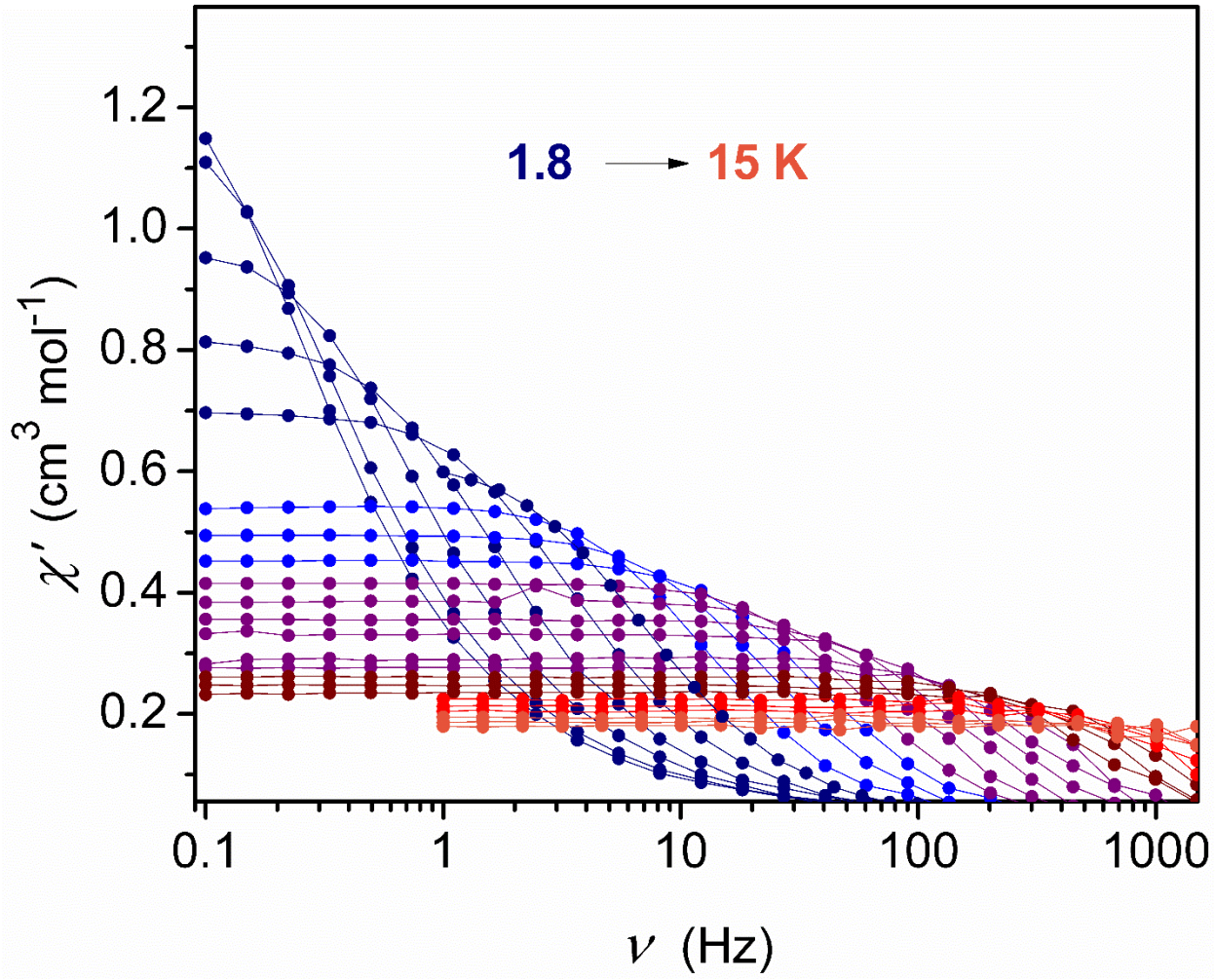

Figure S13. χ' vs. v under 1000 Oe applied DC field for 2.

The temperature was increased in 0.5 K increments from 2 K to 13 K, and 1 K increments from 14 K to 15 K. Data were acquired using an oscillating field of 4 Oe. The lines are guides for the eye.

Fitting of χ''(ν) maxima

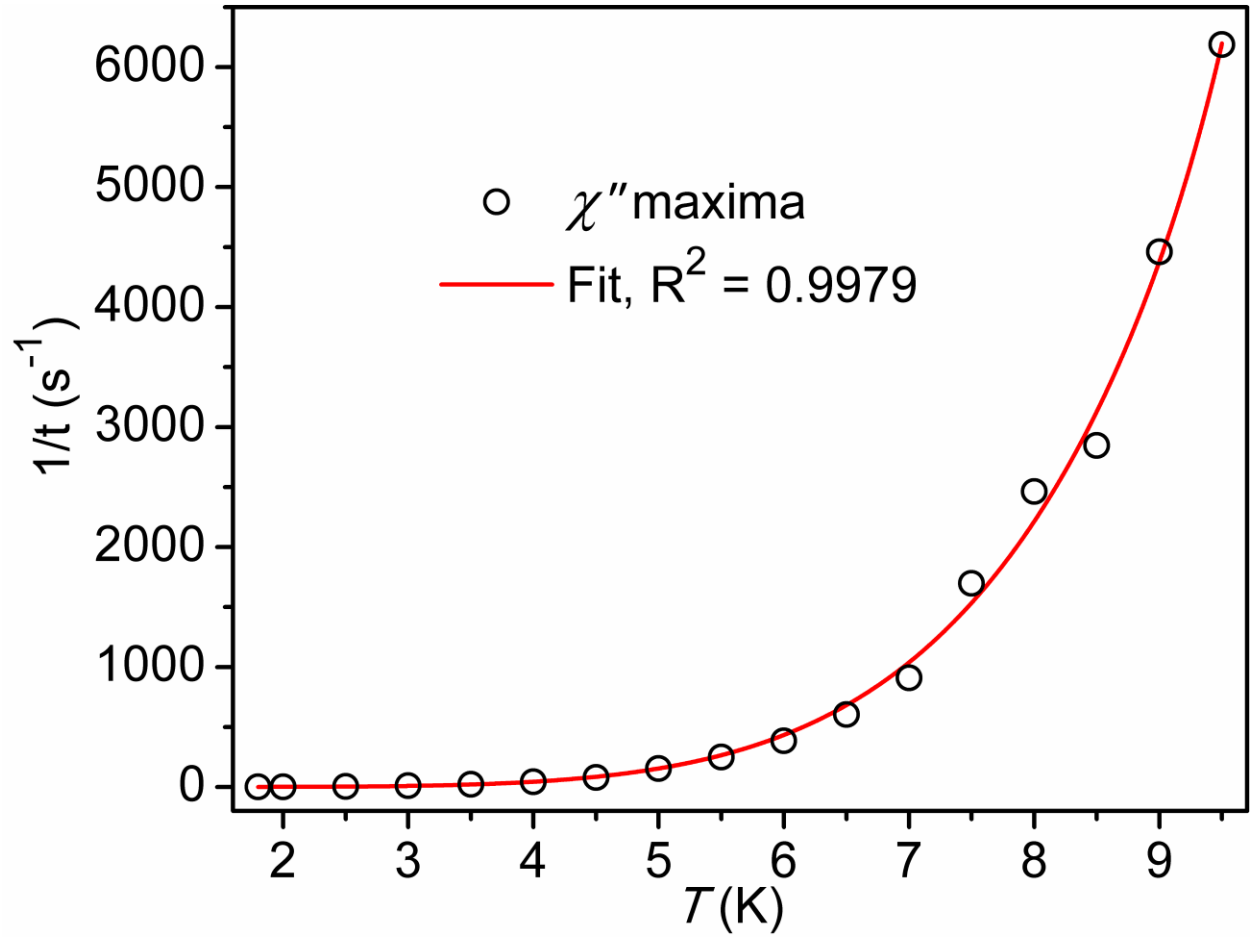

Figure S14. Fit of out-of-phase χ'' maxima (1000 Oe). Fitting the function for Raman and Orbach relaxation processes, $\tau^{-1} = AT^{B} + \tau_0^{-1}e^{(-U/kT)}$, to these data give parameters of A:0.053, B: 5, τ_0: 1.8×10^{-7}, and U: 75.2, with R^2 = 0.9979. Thus, the thermal barrier to relaxation is determined to be 75.2 K. We note that including a term for a direct relaxation process results in a slightly better fit to the curve (R^2 = 0.99812), however the values obtained for these parameters are physically unrealistic, so that term was not included in the final model.

Computations

All calculations used crystal coordinates with adjusted CH and NH bond distances. RC-H sp^3=1.09 Å, RC-H sp^2=1.07 Å, RN-H=1.02 Å. Computations used the 3.03 ORCA electronic structure package.[8] The def2-SVP basis was used[9] and a state averaged (6 quartets, 2 doublets) CAS(7,5) wavefunction was used to define the reference space for the NEVPT2[10] computation of properties.[11]

Table S3. Computed magnetic data.

	1A (bare cation)	2A (bare cation)	2A (with Na,H_2O)	$Co(acac)_2(H_2O)_2$	$Co(acac)_2(H_2O)_2$ ZORA
g_{xx}	1.93	1.31	1.32	1.91	1.91
g_{yy}	2.00	1.34	1.35	2.56	2.55
g_{zz}	3.14	3.45	3.45	2.86	2.85
D (cm^{-1})	-104	-142	-142	81.7	79.2
E/D	0.050	0.020	0.021	0.182	0.189

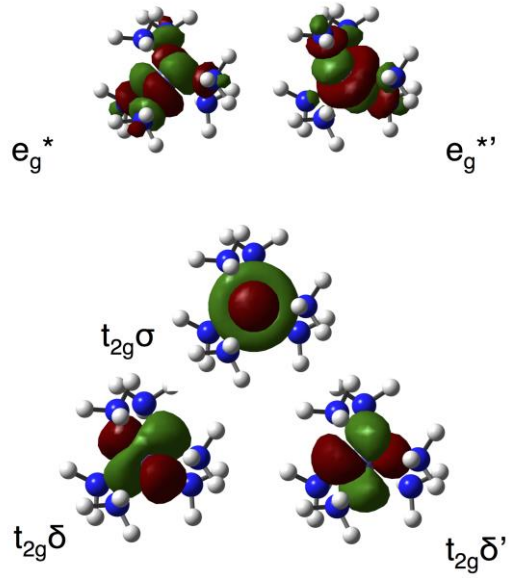

Figure S15. CAS orbitals for a 30˚ distortion.

The orbitals are shown as viewed down the 3-fold rotational (z) axis of the molecule. The 30° distortion angle is defined as the twisting of the ammine planes such that there is a 30° distortion from a perfect trigonal prism (which would be 0°). The “symmetry” labels are intended to assist correlation to orbitals in octahedral coordination geometry.

Discussion. As described succinctly in the literature (ref 35) the sign and value of *D* can be rationalized using the spin−orbit operator, which couples the ground and excited states. When

the excited state results from the excitation between orbitals with the same $|m_l|$ values, the $l_z \bullet s$ operator couples the two orbitals, stabilizing the $M_s = \pm 3/2$ components and giving rise to a negative contribution to the *D* value. When the excited state results from excitation between orbitals with $|\Delta m_l| = 1$, the $l_+ \bullet s^- + l_- \bullet s^+$ operator stabilizes the $M_s = \pm 1/2$ components, which leads to a positive contribution to the *D* value.

At 30˚, the ground state (gs) consists of a doubly occupied $t_{2g}\delta$, a singly occupied $t_{2g}\delta'$ and a doubly occupied $t_{2g}\sigma$ and two singly occupied e_g* orbitals. The nearly degenerate second state (1st es), $t_{2g}\delta^1$, $t_{2g}\delta'^2$, $t_{2g}\sigma^2$, is at 73 cm^{-1}, while the 2nd es at 2500 cm^{-1}, which has both $t_{2g}\delta$ orbitals doubly occupied and the $t_{2g}\sigma$ singly occupied, is too high to contribute to *D*. The lowest two states share m_l values, the largest reduced spin orbital coupling matrix element is $\langle 2|l_z s|1\rangle$ and *D* is negative. By 52.5˚ the dominant configuration for the lowest two states is $t_{2g}\delta^2$, $t_{2g}\delta'^2$, $t_{2g}\sigma^1$. Excitation is dominated by changes in m_l. The largest reduced spin orbital coupling matrix elements are $\langle 1|l_x s|0\rangle$ and $\langle 2|l_y s|0\rangle$, and D is positive.

References

1. A. M. McDaniel, C. M. Klug, M. P. Shores, *Eur. J. Inorg. Chem.*, 2013, 943.

2. J. B. Bialecki, L. H. Yuan, B. Gong, *Tetrahedron*, 2007, **63**, 5460.

3. G. A. Bain, J. F. Berry, *J. Chem. Educ.*, 2008, **85**, 532.

4. N. F. Chilton, R. P. Anderson, L. D. Turner, A. Soncini, K. S. Murray, *J. Comput. Chem.*, 2013, **34**, 1164.

5. *Apex 2*; Bruker Analytical X-Ray Systems, Inc.: Madison, WI, 2008.

6. G. M. Sheldrick *SHELXTL*, *Version 6.14*; Bruker Analytical X-Ray Systems, Inc.: Madison, WI, 1999.

7. L. Chen, J. Wang, J. M. Wei, W. Wernsdorfer, X. T. Chen, Y. Q. Zhang, Y. Song, Z. L. Xue, *J. Am. Chem. Soc.*, 2014, **136**, 12213.

8. F. Neese, The ORCA program system, Wiley Interdiscip. Rev.: Comput. Mol. Sci., 2012, **2**, 73–78.

9. A. Schäfer, H. Horn, R. Ahlrichs, *J. Chem. Phys.*, 1992, **97**, 2571; A. Schäfer, C. Huber, R. Ahlrichs, *J. Chem. Phys.*, 1994, **100**, 5829.

10. C. Angeli, R. Cimiraglia, S. Evangelisti, T. Leininger, J.-P. Malrieu, *J. Chem. Phys.*, 2001, **114**, 10252; C. Angeli, R. Cimiraglia, J.-P. Malrieu, *Chem. Phys. Lett.*, 2001, **350**, 297; C. Angeli, R. Cimiraglia, J.-P. Malrieu, *J. Chem. Phys.*, 2002, **117**, 9138; C. Angeli, S. Borini, M. Cestari, R. Cimigraglia, *J. Chem. Phys.*, 2004, **121**, 4043.

11. D. Ganyushin, F. Neese, *J. Chem. Phys.,* 2013, **138**, 104113; M. Atanasov, J. M. Zadrozny, J. R. Long, F. Neese, *Chem. Sci.*, 2013, **4**, 139; M. Atanasov, D. Ganyushin, D. A. Pantazis, K. Sivalingam, F. Neese, *Inorg. Chem.*, 2011, **50**, 7460.